

Weak, Stochastic Temporal Correlation of Large-Scale Synaptic Input Is a Major Determinant of Neuronal Bandwidth

David M. Halliday

Division of Neuroscience and Biomedical Systems, Institute of Biomedical and Life Sciences, University of Glasgow, Glasgow, G12 8QQ, U.K.

We determine the bandwidth of a model neurone to large-scale synaptic input by assessing the frequency response between the outputs of a two-cell simulation that share a percentage of the total synaptic input. For temporally uncorrelated inputs, a large percentage of common inputs are required before the output discharges of the two cells exhibit significant correlation. In contrast, a small percentage (5%) of the total synaptic input that involves stochastic spike trains that are weakly correlated over a broad range of frequencies exert a clear influence on the output discharge of both cells over this range of frequencies. Inputs that are weakly correlated at a single frequency induce correlation between the output discharges only at the frequency of correlation. The strength of temporal correlation required is sufficiently weak that analysis of a sample pair of input spike trains could fail to reveal the presence of correlated input. Weak temporal correlation between inputs is therefore a major determinant of the transmission to the output discharge of frequencies present in the spike discharges of presynaptic inputs, and therefore of neural bandwidth.

1 Introduction ---

Mammalian central nervous system neurones have extensive dendritic trees (Mel, 1994). The combined effects of large-scale synaptic input to such structures act in several ways, which contribute directly and indirectly to the output discharge of the cell. Bernander, Douglas, Martin, and Koch (1991) and Rapp, Yarom, and Segev (1992) demonstrated that large-scale synaptic activity can alter the integrative properties of a cell by acting to reduce the input resistance and time constant. Bernander et al. (1991) further demonstrated that large-scale background synaptic activity results in an increased sensitivity to highly synchronized inputs. Murthy and Fetz (1994) and Bernander, Koch, and Usher (1994) showed that highly synchronized inputs can modulate the mean firing rate of a cell. Dendrites are known to act as low-pass filters (Rinzel & Rall, 1974), which in terms of populations of synaptic inputs results in a filtering out of higher-frequency components present in

input spike trains (Farmer, Bremner, Halliday, Rosenberg, & Stephens, 1993; Halliday, 1995).

This study examines the response of cells to different strengths of temporal correlations within subpopulations of the total synaptic input. Particular attention is given to an important aspect of neuronal systems: the widespread presence of noise at all levels (Holden, 1976), which results in the random fluctuations in membrane potential observed in intracellular recordings (Calvin & Stevens, 1968) and the stochastic nature of both interspike intervals and the temporal correlation between spike trains. This study includes weak stochastic temporal correlation between presynaptic inputs, in contrast to the highly synchronized form of temporal correlation used in the above studies, where all synchronized inputs always fire together within a narrow time window. The aim is to match natural patterns of correlation more closely (Singer, 1993; Gray, 1994).

We consider first the effects of uncorrelated inputs, where a large percentage of common inputs are required before the two cells exhibit significant correlation. In contrast, for inputs with weak temporal correlation, a small percentage (5–10%) of the total synaptic input can exert a clear influence on the output discharge at frequencies where the inputs are correlated. Preliminary results are presented in Halliday (1998b).

2 Model Description and Parameters

The model is based on a class of cells with extensive dendrites whose morphology and electrophysiology have been widely studied (Cullheim, Fleshman, Glenn, & Burke, 1987; Fleshman, Segev, & Burke, 1988; Rall et al., 1992): spinal motoneurons. Based on these studies, the membrane resistivity, R_m , is $11,000\Omega \cdot \text{cm}^2$, the cytoplasmic resistivity, R_i , is $70\Omega \cdot \text{cm}$, and the membrane capacitance, C_m , is $1.0\mu\text{F}/\text{cm}^2$. Each cell has a spherical soma of $50\mu\text{m}$ diameter with 12 tapered dendrites, 4 each of three types: short, medium, and long. A uniform taper of $0.5\mu\text{m}$ per $100\mu\text{m}$ length is used for dendrite diameters in the distal direction. For each dendrite type, the initial diameters at the soma are 5, 7.5, and $10\mu\text{m}$; the physical lengths are 766, 1258, and $1904\mu\text{m}$; the electrotonic lengths are $L = 0.7, 1.0, \text{ and } 1.5$; and the total membrane areas are 8100, 18,500 and $33,500\mu\text{m}^2$, respectively. Each dendrite is modeled as a sequence of connected cylinders, of fixed electrotonic length of 0.1 unit; the complete cell model has 129 compartments, representing a total membrane area of $248200\mu\text{m}^2$, with 97% of this area in the 12 dendrites. The input resistance of the complete model neurone (including soma and tapered dendrites) to hyperpolarizing current injected at the soma is $4.92M\Omega$, and the time constant is 9.7 msec. The compartmental model provides a model of current flow in dendrites accurate to second order in both space and time (Segev, Fleshman, & Burke, 1989; Mascagni, 1989).

Action potential generation and afterhyperpolarization (AHP) currents are based on the model of Baldissera and Gustafsson (1974). This incorpo-

rates a threshold-crossing mechanism in conjunction with a time-dependent potassium conductance to represent AHP currents. The three-term model for potassium conductances proposed by Baldissera and Gustafsson is reduced to its single dominant term of an exponential function with a time constant of 14 msec. At the low firing rates used in this study, it is not necessary to include the faster-acting conductances. Output spikes are generated when the membrane potential at the soma exceeds the fixed threshold of -55 mV, and the AHP conductance is activated after each output spike. This conductance produces a rapid hyperpolarization of the membrane potential toward the reversal potential of -75 mV. With constant injected current sufficient to induce an output firing rate of 12 spikes/sec, the membrane potential at the soma following each output spike decreases by approximately 12 mV.

Individual excitatory synaptic inputs use a time-dependent conductance change, specified by an alpha function: $g_{syn}(t) = G_s t / \tau e^{-t/\tau}$ (Jack, Noble, & Tsien, 1975), with the time constant for this conductance change set at $\tau = 2e - 04$ sec (Segev, Fleshman, & Burke, 1990), and scaling factor $G_s = 1.19e - 08$, giving a peak conductance change of 4.38 nS at $t = 0.2$ msec. The membrane resting potential is -70 mV, and the reversal potential for excitatory postsynaptic potentials (EPSPs) is -10 mV. When activated at the soma from rest, this conductance generates an EPSP with peak magnitude 100μ V at $t = 0.525$ msec, and a rise time (10% to 90%) and half-width of 0.275 msec, 2.475 msec. The EPSP parameters at the soma when activated in the most distal compartment of the short dendrite ($L = 0.7$) are 52.8μ V at $t = 2.00$ msec, and 0.900, 7.05 msec. When activated in the most distal compartment of the medium dendrite ($L = 1.0$), the EPSP parameters are 40.4μ V at $t = 3.08$ msec, and 1.35, 9.35 msec. Activation in the most distal compartment of the long dendrite ($L = 1.5$) gives EPSP parameters at the soma of 27.1μ V at $t = 4.75$ msec, and a rise time and half-width of 2.08, 11.38 msec.

Presynaptic inputs are spatially distributed uniformly by membrane area over the soma and dendrites. The level of excitation necessary to induce a constant firing rate of around 12 spikes/sec in the model cell is 31,872 EPSPs/sec. This can be achieved by 996 uniformly distributed inputs firing randomly at 32 spikes/sec. In this configuration the soma receives 32 inputs, and each dendrite type (short, medium, and long) receives 33, 74, and 134 synaptic inputs each, distributed by area over the surface of the dendrite. In the examples below, where periodic inputs form part of the total synaptic input, the mean rate and number of inputs are adjusted in tandem to provide the same number of EPSPs/sec acting on each compartment of the model.

3 Data Analysis and Inference of Neural Bandwidth _____

The simulations consist of two cells in which a percentage of the total synaptic input is common to both cells. The cells therefore exhibit a tendency for

correlated discharge, which we use to estimate the range of frequencies in the common input spike trains that are transmitted to the output discharge of the cells. The data analysis methods are those set out in Rosenberg, Amjad, Breeze, Brillinger, and Halliday (1989) and Halliday et al. (1995) for frequency domain analysis of stochastic neuronal data. We use estimates of coherence functions and cumulant density functions to characterize the correlation between the output discharges. Cumulant density functions provide a measure of correlation between spike trains as a function of time; coherence functions provide a measure of correlation as a function of frequency. The cumulant density function, at lag u , between two spike trains (1, 2), denoted by $q_{12}(u)$, can be defined and estimated as the inverse Fourier transform of the cross spectrum:

$$q_{12}(u) = \int_{-\pi}^{\pi} f_{12}(\lambda) e^{i\lambda u} d\lambda,$$

where $f_{12}(\lambda)$ is the cross spectrum between (1, 2) at frequency λ . The corresponding coherence function, $|R_{12}(\lambda)|^2$, can be defined and estimated as the magnitude of the cross spectrum squared normalized by the product of the two auto spectrum:

$$|R_{12}(\lambda)|^2 = \frac{|f_{12}(\lambda)|^2}{f_{11}(\lambda)f_{22}(\lambda)}.$$

For further details including estimation procedures and the setting of confidence limits, see Halliday et al. (1995).

For two identical neurones acted on by a single common input, the estimated coherence between the output discharges is proportional to the product of the input spectrum with the squared magnitude of the transfer function (defined as the ratio of the cross spectrum and input spectrum) for this single input (Rosenberg, Halliday, Breeze, & Conway, 1998). Using random, or Poisson, common spike train inputs allows the bandwidth of the cell input-output transfer function to be inferred from the estimated coherence between the output discharges of the two cells. We use a similar approach in this study, except that we are dealing with a population of common inputs to the two cells. This method has the advantage of being independent of the number of inputs applied to the cell; the application and interpretation is the same for 1 or 1000 common inputs. The estimation of a multivariate transfer function for a cell with several hundred inputs is not practical. In addition, the two-cell method will also be useful when nonlinear mechanisms are involved in synaptic transmission. Our concern is with the presence of common frequency components in the two output discharges; since the common inputs have the same effect on both cells, the two-cell model will also be useful when linear and nonlinear transformations of input signals occur.

Some of the simulations use presynaptic input spike trains that are periodic. We interpret a distinct peak in the estimated coherence between the

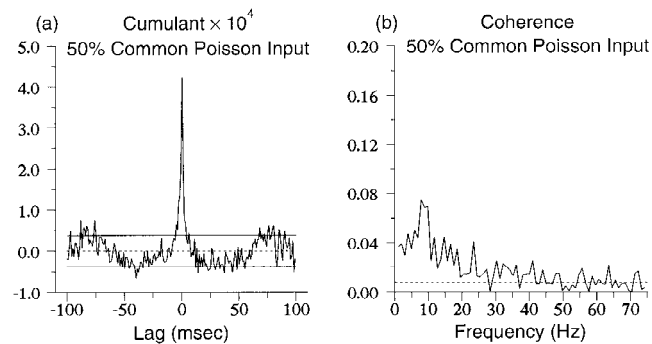


Figure 1: Synchronized discharge in the two-cell model induced by 50% common inputs with Poisson discharges. (a) Cumulant density estimate. Dashed and solid horizontal lines are expected value and upper and lower 95% confidence limits, respectively, based on assumption of independence. (b) Coherence estimate. Dashed horizontal line is upper 95% confidence limit based on assumption of independence. Results estimated from 400 seconds of data.

two output discharges at the frequency of the periodicity to indicate that this frequency is within the bandwidth of the cell for that particular input configuration. This inference uses an important property of a Fourier-based analytical framework: that distinct frequencies persist within a (linear) system (Brillinger, 1974), and can be detected as a periodic correlation between an input and an output, or between two outputs.

Inferring the properties of common inputs to neurones from the estimated correlation between their output discharges is a well-established approach in both modeling of neural systems (Perkel, Gerstein, & Moore, 1967; Moore, Segundo, Perkel, & Levitan, 1970; Rosenberg et al., 1998) and neurophysiology (Farmer et al., 1993).

4 Results

4.1 Uncorrelated Inputs. With both cells acted on by 996 inputs, each activated by a Poisson spike train of rate 32 spikes/sec, and no common inputs, both cells fire with a mean rate of around 12 spikes/sec, and, as expected, their output discharges are uncorrelated. When 50% of the inputs are applied commonly, the cells share 15,936 EPSPs/sec, and their output discharges exhibit a tendency for synchronous discharge. This results in a peak at time zero in the time domain correlation, (see Figure 1a) estimated as a cumulant density function (Halliday et al., 1995). In the frequency domain, significant correlation is present at frequencies up to around 50 Hz in the estimated coherence (see Figure 1b). Therefore the bandwidth of this configuration, which reflects the ability of 50% of the synaptic inputs acti-

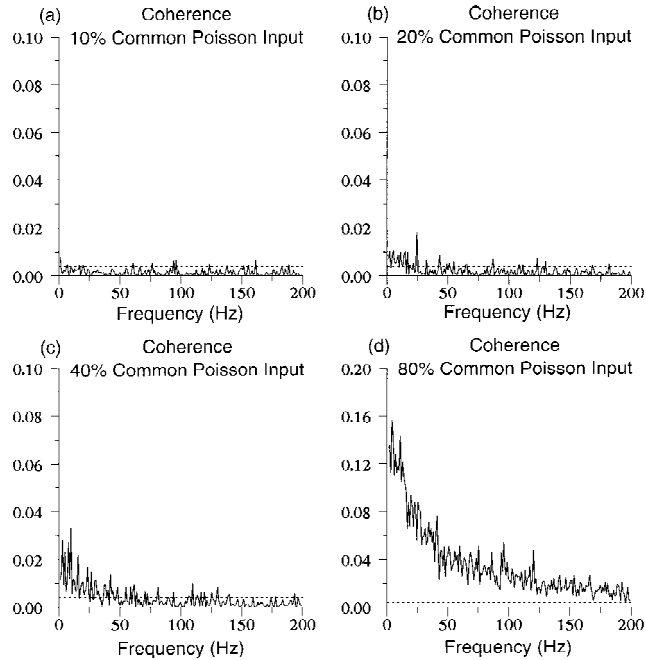


Figure 2: Response of two-cell model to different percentages of common Poisson inputs. Estimated coherence between output discharges for (a) 10%, (b) 20%, (c) 40%, and (d) 80% common Poisson inputs applied uniformly over entire dendritic tree. Dashed horizontal lines are confidence limits as described for Figure 1. Results estimated from 800 seconds of data for each configuration.

vated by random spike trains to influence the output discharge, is around 50 Hz.

In Figure 2 are shown coherence estimates between the output discharges when each cell receives the same number of EPSPs/sec as above, except that the percentage of common EPSPs/sec is varied from 10% to 80%. These common inputs are activated by Poisson spike trains, their location is distributed uniformly by area over the cell body and dendrites, and they have the same location in both cells. The coherence estimate with 10% common inputs (see Figure 2a) has no significant features; therefore, the combined effect of 10% of the total synaptic input is insufficient to exert any influence on the timing of output spikes. The configuration with 80% common input (see Figure 2d) has a coherence estimate with significant values up to frequencies in excess of 200 Hz. The bandwidth of this configuration is therefore above 200 Hz. The bandwidth of the neurone therefore depends on the percentage of the total synaptic input that is considered to provide the input. Coherence es-

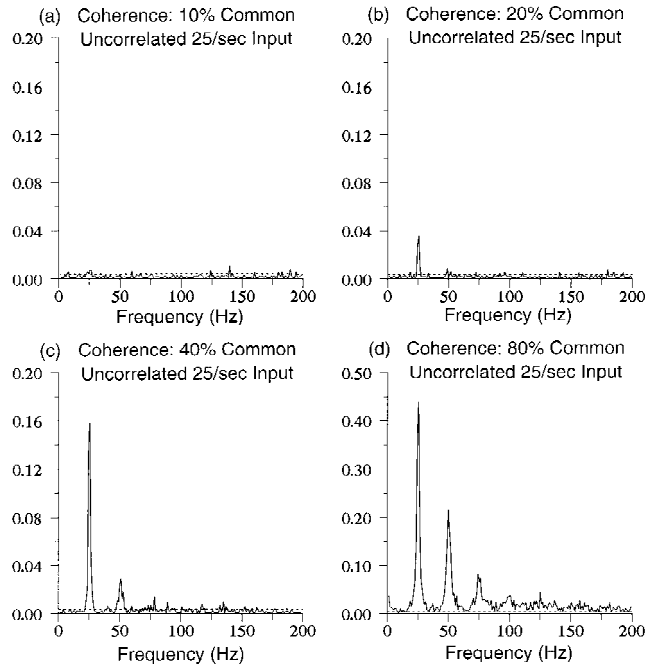


Figure 3: Response of two-cell model to different percentages of common uncorrelated periodic 25 spikes/sec inputs. Estimated coherence between output discharges for (a) 10%, (b) 20%, (c) 40%, and (d) 8% common inputs applied uniformly over entire dendritic tree. Dashed horizontal lines are confidence limits as described for Figure 1. Results estimated from 800 seconds of data for each configuration.

estimates provide a normative measure of association on a scale from 0 to 1 (Rosenberg et al., 1989; Halliday et al., 1995). The peak coherence between the two output discharges with 80% common synaptic input is 0.15. Thus, even with 80% common synaptic input to the two cells, the discharge of one cell can predict a maximum of 15% of the variability in the discharge of the companion cell.

The above configurations using Poisson spike trains are equivalent to probing a continuous system with a white noise signal; both types of signal have a flat spectral estimate. Many neural systems have pathways that carry periodic spike trains. In addition, there has been recent interest in the role of rhythmic neuronal activity in neural integration (Singer, 1993; Gray, 1994). This raises the question of whether the bandwidths inferred from the coherence estimates in Figure 2 are valid for spike train inputs that contain distinct periodicities. This is explored in Figure 3, which shows

coherence estimates, with the common inputs activated by periodic spike trains with a mean rate of 25 spikes/sec and a coefficient of variation (COV) of 0.1. As above, in determining the number of inputs, the total number of EPSPs/sec acting on each compartment remained fixed. For example, the soma of each cell receives 1024 EPSPs/sec, which with 10% common synaptic input consists of 4 periodic inputs firing at 25 spikes/sec common to both cells and 37 random inputs firing at 25 spikes/sec applied independently to each cell. Figure 3 demonstrates that the behavior of the simulation in response to a varying percentage of common periodic inputs is similar to that for random inputs. With only 10% of the inputs firing at 25 spikes/sec there is no significant coherence at 25 Hz (see Figure 3a). An increasing percentage of inputs firing at 25 spikes/sec results in an increase in the magnitude of the coherence estimate at 25 Hz, and also an increase in the range of frequencies present, seen as peaks at harmonics of the 25 Hz input.

4.2 Correlated Inputs. The simulations suggest that populations of synaptic inputs activated by uncorrelated spike trains that constitute less than 20% of the total synaptic input to a cell are unlikely to exert any influence on the timing of output spikes. Next we explore the response to input spike trains that are themselves correlated. Each spike train is generated using an integrate-and-fire encoder, and the resulting correlation within each population of common inputs is both weak and stochastic in nature (Halliday, 1998a). These integrate-and-fire encoders are much simpler than the detailed conductance-based compartmental neurone model. They are used to generate correlated spike trains and are not intended to represent presynaptic circuitry acting on motoneurons.

First we examine the response of the paired motoneurone model to a population of common inputs with the same firing rate (32 spikes/sec) and COV (1.0) as the Poisson inputs used in Figures 1 and 2, except they are weakly correlated over a broad range of frequencies. These inputs are generated using the spike generators described in Halliday (1998a), with the temporal correlation generated by a single Poisson spike train of rate 32 spikes/sec as common input to all spike generators. The resulting strength of correlation between sample pairs of spike trains is broadband and weak. Due to this weak temporal correlation, analysis of a sample pair of spike trains of duration 100 seconds can fail to reveal any significant correlation between inputs (Halliday, 1998a). However, combined analysis of 20 sample pairs of 100 seconds duration using the technique of pooled coherence (Amjad, Halliday, Rosenberg, & Conway, 1997; Halliday, 1998a) reveals correlation within the population of inputs up to 100 Hz, with a maximum estimated coherence of 0.013. Figure 4a shows the coherence estimate between the two output discharges, with 10% common input supplied by 100 of these correlated inputs distributed uniformly by area as before. This estimate is similar to that obtained with 60% common Poisson inputs (not

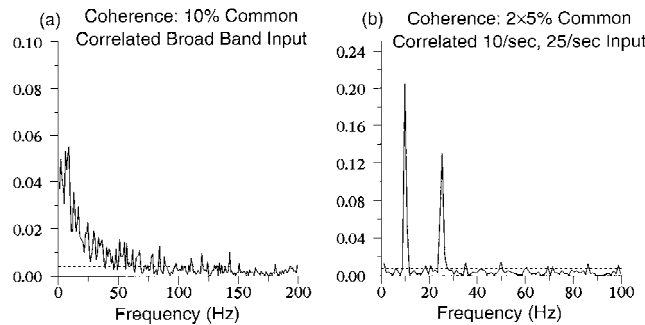


Figure 4: Response of two-cell model to populations of inputs with weak temporal correlation. Estimated coherence between output discharges for (a) 10% common correlated broadband inputs and (b) 5% common correlated periodic inputs at 10 spikes/sec and 5% common correlated periodic inputs at 25 spikes/sec applied uniformly over entire dendritic tree. Dashed horizontal lines are confidence limits as described for Figure 1. Results estimated from 800 seconds of data in (a) and 400 seconds of data in (b).

shown; cf. Figures 2c and 2d). Weakly correlated inputs exert a significantly stronger influence on the output discharge of the cell than uncorrelated inputs. The configuration with 10% weakly correlated inputs has a bandwidth in excess of 100 Hz, in contrast to the configuration with 10% uncorrelated inputs, which has no significant effect on the timing of output spikes.

Next we examine the effects of applying two sets of common periodic spike trains, with each set assigned 5% of the total number of EPSPs/sec acting on the cells, and consisting of 160 inputs firing at 10/sec with COV 0.1, and 64 inputs firing at 25 spikes/sec, with COV 0.1. These spike trains have a similar strength of correlation as the broadband inputs above, except the correlation is at the firing frequency in each set of 10 Hz and 25 Hz, respectively (Halliday, 1998a). The coherence estimate between the two output discharges has clear peaks at 10 Hz and 25 Hz. Thus, the output discharge supports both periodicities present in the two populations of weakly correlated common inputs. The 5% of inputs at 25/sec induce a peak coherence similar to that in Figure 3c for 40% common uncorrelated 25 spikes/sec inputs. A small percentage of weakly correlated periodic inputs are able to exert an influence on the timing of output spikes whose relative magnitude is far in excess of the percentage of input EPSPs involved. Weak stochastic correlation between inputs (which may not be detected) is converted into stronger correlation between outputs. A small change in the temporal correlation structure of a subset of the total synaptic input, without any alteration in mean firing rate, can alter the bandwidth of the cells.

5 Discussion

The main finding of this study is the dynamic nature of the cell bandwidth, which for a fixed level of synaptic excitation (EPSPs/sec), exhibits systematic changes in response to changes in the numbers of presynaptic inputs considered to provide the input signal and their temporal correlation characteristics. For uncorrelated inputs, neural bandwidth is determined by the percentage of the total synaptic input that is considered to provide the input signal. Populations that constitute less than 10% of the total synaptic input have no significant influence on the output discharge (see Figures 2a and 3a). In contrast, weak temporal correlation within 5–10% of the total synaptic input has considerable influence on the timing of output spikes (see Figure 4). Correlation between the output discharges occurs at the frequencies at which inputs are correlated. Weak temporal correlation between inputs is converted into stronger correlation between outputs.

The question of neural bandwidth has been previously addressed. Farmer et al. (1993) used a similar two-cell simulation of a point neurone model and found that EPSPs with longer rise times and half-widths acted to filter out higher-frequency components. Based on a two-cell model with 96.5% of the total inputs common to both cells, they concluded that the bandwidth of their point neurone model was in excess of 250 Hz. Using a two-cell model of a motoneurone plus single attached dendrite with 75% of the total synaptic input common to both cells, Halliday (1995) concluded that a distal input location could result in a bandwidth of around 50 Hz. The findings of this study are consistent with these previous results and show that these different estimates of the cell bandwidth result from the different percentages of common inputs applied. The classical view of the input-output relationship for motoneurons is that over a wide range of discharge rates, the steady-state discharge rate is determined by a simple linear relation that is proportional to the effective synaptic current input to the cell (Binder, Heckman, & Powers, 1993). This study is concerned with spatial temporal interactions on a millisecond timescale, which for large-scale synaptic input results in membrane potential fluctuations (Calvin & Stevens, 1968). It is the random nature of these fluctuations, and the interactions between the populations of common and independent inputs, that produces the modulation of neural bandwidth for the same level of average excitation.

Two previous studies of the effects of input synchrony have concentrated on variations in mean firing rate (Murthy & Fetz, 1994; Bernander et al., 1994). Both sets of authors found that increased synchronization led to a decrease in output firing rate. The proposed mechanism was an "overcrowding" effect where excess depolarizing input above that required to fire the cell was effectively wasted during the refractory period. For the present simulations the average output firing rate was 12.32 spikes/sec for the Poisson input configurations (see Figures 1 and 2), 12.37 spikes/sec for the weakly correlated broadband inputs (see Figure 4a), and 12.16 spikes/sec for the

weakly correlated periodic inputs (see Figure 4a). This study differs from these in the use of weak, stochastic correlated inputs. Generation of spike trains using integrate-and-fire encoders results in patterns of correlation that mimic more realistically natural patterns of correlation, rather than the highly synchronized inputs used by Murthy and Fetz (1994) and Bernander et al. (1994), where all correlated inputs fire synchronously with probability 1 in a narrow time window.

Bernander et al. (1991) and Rapp et al. (1992) found that large-scale synaptic activity can alter the basic characteristics of a cell, resulting in a reduction in cell input resistance and time constant. The present model exhibits similar behavior; when excited by 31,872 EPSPs/sec, the input resistance is 3.8 M Ω , the time constant is 6.45 msec, and the average membrane potential is -55.1 mV. This compares with 4.9 M Ω , 9.7 msec and -70 mV with no synaptic inputs.

Bernander et al. (1991) concluded that large-scale background synaptic activity also resulted in increased sensitivity to synchronized inputs, which they demonstrated by contrasting the cell response to 150 inputs that were either exactly synchronized every 25 msec or distributed throughout time. There are two differences in the methods of this study. Bernander et al. (1991) and Rapp et al. (1992) replaced individual background synaptic conductances with a time-averaged constant calculated to provide the same average level of excitation to each compartment. This study is concerned with the stochastic nature of neuronal spike trains and therefore models the time course of each individual synaptic input in full for all synaptic inputs to both cells. In the absence of any other synaptic inputs, a constant background conductance will result in a constant value of membrane potential, which will not exhibit the random fluctuations observed in intracellular recordings (Calvin & Stevens, 1968; see Bernander et al., 1991, Figure 1c). This will bias the response of the model in favor of any synaptic inputs that are applied, since these will be the only source of membrane potential fluctuations and the cell will always respond with an increased depolarization to excitatory inputs. This is in contrast to this model, where the synaptic inputs that provide the input signal interact and compete with the background synaptic inputs on a millisecond timescale. Theoretical studies have indicated that the addition of noise to a system can result in an improved signal-to-noise ratio, particularly for periodic signals in the presence of noise (Wiesenfeld & Moss, 1995; Beuzukov & Vodyanoy, 1997). In such a case it is important to model the stochastic nature of all inputs to the cell; indeed in the light of this work on stochastic resonance, the presence of stochastic background synaptic activity may contribute to the extreme sensitivity of the cell to other temporally correlated synaptic inputs. The second difference between this study and that of Bernander et al. (1991) is in the form of correlated inputs. Bernander et al. (1991) used precisely synchronized inputs, in contrast to the weak, stochastic temporal correlation used in our populations of inputs. This temporal correlation is sufficiently weak that examination of a sample

pair of spike trains selected from the population may fail to reveal the presence of any correlation (Halliday, 1998a). Despite the presence of large-scale background activity, the model cell is able to detect the presence of weak, stochastic temporal correlation in a small fraction of the total input, without any change in the overall level of excitation (EPSPs/sec). This high selectivity to small changes in the temporal characteristics of subpopulations of the total synaptic input suggests that weak, stochastic temporal correlation between presynaptic inputs is a major determinant of neural bandwidth.

The results of this study are also relevant to studies considering the relative merits of rate coding, coincidence detection, and temporal integration as mechanisms involved in neural coding (Shadlen & Newsome, 1994, 1995, 1998; Softky, 1995; König, Engel, & Singer, 1996), which have led to the view that temporal integration, where many PSPs contribute to the generation of each output spike, will not preserve temporal coding in input spike trains (Shadlen & Newsome, 1994; König et al., 1996). In the simulations here, around 2666 EPSPs contribute to each spike; therefore temporal integration would appear to be the dominant mode of operation. The presence of weak stochastic temporal correlation in 5–10% of the total synaptic input allows these inputs to exert a strong influence on the timing of output spikes, allowing the temporal coding in the inputs to be transmitted to the output discharges. This result is not consistent with the suggestion that temporal information will not propagate through neurones whose mode of operation is temporal integration. An alternative mode of operation proposed for neurones is coincidence detection (Abeles, 1982; Softky, 1994; König et al., 1996). It is not clear that this is an appropriate mechanism to describe the present simulations, where weakly correlated inputs are distributed over the extensive dendritic tree, with propagation delays of up to 5 ms for distal inputs to arrive at the somatic spike generation site. In addition, the weak and stochastic nature of the correlation structure in the common inputs does not produce reliable coincidences in the input spike trains (Halliday, 1998a), but a diffuse temporal correlation distributed across all the spike trains in each population. We therefore suggest that the mode of operation of the present neurones is temporal integration with correlation detection.

The results also demonstrate that correlation between neurones does not require any alteration in output firing rates (deCharms & Merzenich, 1996; Riehle, Grün, Diesmann, & Aertsen, 1997). Weak correlation between inputs results in stronger correlation between outputs; reciprocal connections in networks of neurones may provide a means of sustaining these oscillations. In such networks, conduction delays are an important factor (König & Schillen, 1991); however, in the present data, dendritic conduction delays of up to 5 ms do not affect the ability of the neurone to detect temporal correlation between inputs. One unresolved issue in cortical signaling is the variability exhibited in neuronal discharges, which have a COV ~ 1.0 (Softky & Koch, 1993; Shadlen & Newsome, 1994, 1998). In this study the neurones

have a regular output discharge. However, all inputs in the example in Figure 4a. have a COV ~ 1.0 , yet the cell is sensitive to weak stochastic temporal correlation between inputs distributed over the dendritic tree. Further simulation studies are necessary to ascertain if weak stochastic temporal correlation in populations of inputs contributes to the variability in cortical neurone discharges.

Acknowledgments

This research was undertaken initially at the Information Science Division, NTT Basic Research Labs, Musashino, Tokyo. Completion was supported in part by grants from the Joint Research Council/HCI Cognitive Science Initiative and the Wellcome Trust (036928; 048128).

References

- Abeles, M. (1982). Role of cortical neuron: Integrator or coincidence detector? *Isr. J. Med. Sci.*, *18*, 83–92.
- Amjad, A. M., Halliday, D. M., Rosenberg, J. R., & Conway, B. A. (1997). An extended difference of coherence test for comparing and combining several independent coherence estimates—theory and application to the study of motor units and physiological tremor. *Journal of Neuroscience Methods*, *73*, 69–79.
- Baldissera, F., & Gustafsson, B. (1974). Afterhyperpolarization conductance time course in lumbar motoneurons of the cat. *Acta Physiologica Scandinavica*, *91*, 512–527.
- Bernander, Ö., Douglas, R. J., Martin, K. A. C., & Koch, C. (1991). Synaptic background activity influences spatiotemporal integration in single pyramidal cells. *Proceedings of the National Academy of Sciences*, *88*, 11569–11573.
- Bernander, Ö., Koch, C., & Usher, M. (1994). The effect of synchronized inputs at the single neuron level. *Neural Computation*, *6*, 622–641.
- Bezrukov, S. M., & Vodyanoy I. (1997). Stochastic resonance in non-dynamical systems without response thresholds. *Nature*, *385*, 319–321.
- Binder, M. D., Heckman, C. J., & Powers, R. K. (1993). How different afferent inputs control motoneuron discharge and the output of the motoneuron pool. *Current Opinion in Neurobiology*, *3*, 1028–1034.
- Brillinger, D. R. (1974). Fourier analysis of stationary processes. *Proceedings of the IEEE*, *62*, 1628–1643.
- Calvin, W. H., & Stevens, C. F. (1968). Synaptic noise and other sources of randomness in motoneuron interspike intervals. *Journal of Neurophysiology*, *31*, 574–587.
- Cullheim, S., Fleshman, J. W., Glenn, L. L., & Burke, R. E. (1987). Membrane area and dendritic structure in type-identified triceps surae alpha motoneurons. *Journal of Comparative Neurology*, *255*, 68–81.
- deCharms, R. C., & Merzenich, M. M. (1996). Primary cortical representation of sounds by the coordination of action potential timing. *Nature*, *381*, 610–613.

- Farmer, S. F., Bremner, F. D., Halliday, D. M., Rosenberg, J. R., & Stephens, J. A. (1993). The frequency content of common synaptic inputs to motoneurons studied during voluntary isometric contraction in man. *Journal of Physiology*, *470*, 127–155.
- Fleshman, J. R., Segev, I., & Burke, R. E. (1988). Electrotonic architecture of type-identified (-motoneurons in the cat spinal cord. *Journal of Neurophysiology*, *60*, 60–85.
- Gray, C. M. (1994). Synchronous oscillations in neuronal systems: Mechanisms and functions. *Journal of Computational Neuroscience*, *1*, 11–38.
- Halliday, D. M. (1995). Effects of electronic spread of EPSPs on synaptic transmission in motoneurons—A simulation study. In A. Taylor, M. H. Gladden, & R. Durbaba (Eds.), *Alpha and gamma motor systems* (pp. 337–339). New York: Plenum.
- Halliday, D. M. (1998a). Generation and characterization of correlated spike trains. *Computers in Biology and Medicine*, *28*, 143–152.
- Halliday, D. M. (1998b). Weak, stochastic temporal correlation of large scale synaptic input can modulate neuronal bandwidth. *Society for Neuroscience Abstracts*, *24*, 1151.
- Halliday, D. M., Rosenberg, J. R., Amjad, A. M., Breeze, P., Conway, B. A., & Farmer, S. F. (1995). A framework for the analysis of mixed time series/point process data—Theory and application to the study of physiological tremor, single motor unit discharges and electromyograms. *Progress in Biophysics and Molecular Biology*, *64*, 237–278.
- Holden, A. V. (1976). *Models of the Stochastic Activity of Neurones*. Berlin: Springer Verlag.
- Jack, J. J. B., Noble, D., & Tsien, R. W. (1975). *Electrical current flow in excitable cells* (2nd ed.). Oxford: Clarendon Press.
- König, P., Engel, A. K., & Singer, W. (1996). Integrator or coincidence detector? The role of the cortical neuron revisited. *TINS*, *19*, 130–137.
- König, P., & Schillen, T. B. (1991). Stimulus-dependent assembly formation of oscillatory responses. I. Synchronization. *Neural Computation*, *3*, 155–166.
- Mascagni, M. V. (1989). Numerical methods for neuronal modeling. In C. Koch & I. Segev (Eds.), *Methods in neuronal modeling: From synapses to networks*. (pp. 439–484). Cambridge, MA: MIT Press.
- Mel, B. W. (1994). Information processing in dendritic trees. *Neural Computation*, *6*, 1031–1085.
- Moore, G. P., Segundo, J. P., Perkel, D. H., & Levitan, H. (1970). Statistical signs of synaptic interaction in neurones. *Biophysical Journal*, *10*, 876–900.
- Murthy, V. N., & Fetz, E. E. (1994). Effects of input synchrony on the firing rate of a three conductance cortical neuron model. *Neural Computation*, *6*, 1111–1126.
- Perkel, D. H., Gerstein, G. L., & Moore, G. P. (1967). Neuronal spike trains and stochastic point processes. II. Simultaneous spike trains. *Biophysical Journal*, *7*, 419–440.
- Rall, W., Burke, R. E., Holmes, W. R., Jack, J. J. B., Redman, S. J., & Segev, I. (1992). Matching dendritic neuron models to experimental data. *Physiological Reviews*, *72* (Suppl.), S159–S186.

- Rapp, M., Yarom, Y., & Segev, I. (1992). The impact of parallel fiber background activity on the cable properties of cerebellar Purkinje cells. *Neural Computation*, 4, 518–533.
- Riehle, A., Grün, S., Diesmann, M., & Aertsen, A. (1997). Spike synchronization and rate modulation differentially involved in motor cortical function. *Science*, 278, 1950–1953.
- Rinzel, J., & Rall, W. (1974). Transient response to a dendritic neuron model for current injected at one branch. *Biophysics*, 14, 759–789.
- Rosenberg, J. R., Amjad, A. M., Breeze, P., Brillinger, D. R., & Halliday, D. M. (1989). The Fourier approach to the identification of functional coupling between neuronal spike trains. *Progress in Biophysics and Molecular Biology*, 53, 1–31.
- Rosenberg, J. R., Halliday, D. M., Breeze, P., & Conway, B. A. (1998). Identification of patterns of neuronal activity—partial spectra, partial coherence, and neuronal interactions. *Journal of Neuroscience Methods*, 83, 57–72.
- Segev, I., Fleshman, J. R., & Burke, R. E. (1989). Compartmental models of complex neurons. In C. Koch & I. Segev (Eds.), *Methods in neuronal modeling: From synapses to networks* (pp. 63–96). Cambridge, MA: MIT Press.
- Segev, I., Fleshman, J. R., and Burke, R. E. (1990). Computer simulations of group Ia EPSPs using morphologically realistic models of cat a-motoneurons. *Journal of Neurophysiology*, 64, 648–660.
- Shadlen, M. N., & Newsome, W. T. (1994). Noise, neural codes and cortical organization. *Current Opinion in Neurobiology*, 4, 569–579.
- Shadlen, M. N., & Newsome, W. T. (1995). Is there a signal in the noise? *Current Opinion in Neurobiology*, 5, 248–250.
- Shadlen, M. N., & Newsome, W. T. (1998). The variable discharge of cortical neurons: Implications of connectivity, computation and information coding. *Journal of Neuroscience*, 18, 3870–3896.
- Singer, W. (1993). Synchronization of cortical activity and its putative role in information processing and learning. *Annual Review of Physiology*, 55, 349–374.
- Softky, W. R. (1994). Sub-millisecond coincidence detection in active dendritic trees. *Neuroscience*, 58, 13–41.
- Softky, W. R. (1995). Simple versus efficient codes. *Current Opinion in Neurobiology*, 5, 239–247.
- Softky, W. R., & Koch, C. (1993). The highly irregular firing of cortical cells is inconsistent with temporal integration of random EPSPs. *Journal of Neuroscience*, 13, 334–350.
- Wiesenfeld, K., & Moss, F. (1995). Stochastic resonance and the benefits of noise—from ice ages to crayfish and squids. *Nature*, 373, 33–36.